JOURNAL OF GEOPHYSICAL RESEARCH, VOL. 94, NO. A3, PAGES 2405–2415, MARCH 1, 1989

Tool Kit for Antennae and Thermal Noise Near the Plasma Frequency

NICOLE MEYER-VERNET AND CLAUDE PERCHE

Observatoire de Paris, Departement Recherche Spatiale, Meudon, France

This paper provides the essential tools for deriving quickly the quasi-thermal noise spectrum or the impedance of a given electric antenna near the plasma frequency, for calibration or diagnosis in space plasmas. We give simple analytical expressions and numerical results for either wire or sphere dipoles in an isotropic plasma with one or two Maxwellian electron populations. We include the contribution of the particles collected and/or emitted by the antenna surface. We also indicate some modifications brought about by using more complicated antenna geometries, and a drifting or a magnetized plasma. Finally, we give some conclusions for antenna design or data interpretation in plasma wave experiments.

1 INTRODUCTION

When a passive electric antenna is immersed in a stable plasma, the thermal motion of the ambient electrons and ions produces fluctuations of the electric potential at the antenna terminals. This (quasi) thermal noise can be calculated as a function of the plasma particle velocity distribution functions. Conversely, the spectroscopy of that noise can be used for plasma diagnosis. In any case, this is a ubiquitous phenomenon encountered by any sensitive radio or plasma wave experiment.

This noise was first studied 20 years ago [*Andronov*, 1966; *De Pazzis*, 1969; *Fejer and Kan*, 1969]. Rather ironically, when it was subsequently detected in the solar wind and in planetary magnetospheres, it was generally attributed to "new" electromagnetic emissions or to plasma instabilities (see for instance *Brown* [1973], *Shaw and Gurnett* [1975], *Harvey et al.* [1979], and *Birmingham et al.* [1981]).

Since then, some extensions and applications have been performed [*Meyer-Vernet*, 1979; *Hoang et al.*, 1980; *Couturier et al.*, 1981; *Sentman*, 1982; *Meyer-Vernet*, 1983*a*; *Steinberg and Hoang*, 1986; *Meyer-Vernet et al.*, 1986*a*]; in particular it has been shown that the spectrum measured in the solar wind is very close to the theoretical one. The recent diagnosis of the plasma tail of comet Giacobini-Zinner by thermal noise spectroscopy [*Meyer-Vernet et al.*, 1986*b*,*c*] has proved that, in cold plasmas, this technique yields better results than conventional plasma analyzers. In any case, the knowledge of this noise provides the reference level for radio and plasma wave experiments.

Why did some investigators not recognize this noise when they observed it? Even worse, why did they incorrectly reject this "Occam's razor" interpretation while using correct plasma physics? The main reason is that their antennae were larger than the plasma wavelengths, so that the usual "hand-waving" arguments were erroneous.

The purpose of this paper is to provide the main tools (physical insight, analytical formulae, and numerical results) for calculating the quasi-thermal noise and using it for diagnosis in space plasmas. We give new results, but in order that this toolkit be self-contained, we also include some results published elsewhere in a less "ready-to-use" form. Unless otherwise stated, we use SI units.

Paper number 88JA03265.
0148-0227/89/88JA-03265$05.00

2 THERMAL NOISE ON THE CORNER OF A SLATE

Approximate expressions for the thermal noise spectrum can be obtained from a very simple analysis based on elementary physics. This cannot replace exact results, but provides a physical insight which is essential in the difficult art of choosing the correct approximation in complicated practical cases.

2.1 *Antenna Physics*

The two main types of electric dipoles are thin wires and small spheres (Figure 1). What is the difference between them for measuring longitudinal fields?

With two small spheres, we measure the difference of potential between two points separated by L (along the **Oz** axis): this favours wave vectors satisfying $k_z L \geq 1$. This is not true for a wire antenna, because the potential of each wire of length L is a mean along L: then, only wave vectors $k_z \approx 1/L$ are favoured, and the response decreases roughly as $1/kL$ for larger L.

This fact has two important consequences.

First, although both antennae are equivalent for $kL \ll 1$, there is an optimum length for the wire dipole while the signal on the sphere dipole is length independent (and much larger than that on the wire dipole) if $kL \gg 1$.

Second, suppose that the (longitudinal) field to be measured is anisotropic, being for instance maximum along a certain direction **D**. For which antenna direction **Oz** will the response be maximum? The naive answer is, when **Oz** is parallel to **D**. But if the antenna is a long ($kL \gg 1$) wire dipole, the correct answer is instead, when **Oz** is perpendicular to **D**. Indeed, the field (or **k**) direction for which the sensitivity is maximum satisfies $k_z L \approx 1$; thus if $kL \gg 1$, $k_z/k \approx 1/kL \ll 1$, which corresponds to **k** nearly perpendicular to **Oz**.

2.2 *Plasma Physics*

At frequencies of the order of magnitude of the plasma frequency, the thermal noise is just the power spectrum of the potential induced on the antenna by the plasma electron thermal motion. In the Vlasov framework, the plasma can be thought of as an assembly of "dressed" "test" particles moving in straight lines in the absence of a static magnetic field.

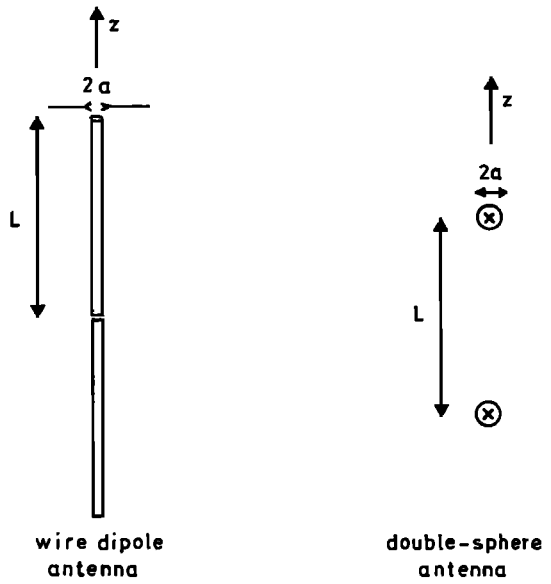

Fig. 1. Antenna geometries.

The following elementary properties of this dressing are necessary (and sufficient) to estimate the thermal noise:

1. For large time scales (or frequencies $\omega < \omega_p$), the particle charge is (Debye) shielded at a distance L_D.

2. For small time scales (or $\omega \gg \omega_p$), the particles have not enough time to dress.

3. For $\omega \approx \omega_p$, there are longitudinal plasma waves of wave number $k_p \approx \left(\omega^2/\omega_p^2 - 1\right)^{1/2}/3^{1/2}L_D$.

2.3 *On Being Large*

Consider a sphere dipole antenna (Figure 1) much longer than the plasma Debye length, namely $L \gg L_D$.

First, what happens if $\omega < \omega_p$? The two spheres see uncorrelated signals, so that the noise is just twice that seen by one sphere. One sphere only sees the electrons as they pass at a distance $r \leq L_D$; let an electron pass with a velocity v_T and an impact parameter $p \leq L_D$: it produces a short potential pulse of duration $L_D/v_T \approx 1/\omega_p$ and amplitude $V \approx e/(4\pi\epsilon_0 p)$. Taking the power spectrum and summing over the event rate $\approx \pi L_D^2 n v_T$ yields approximately the white spectrum given in Table 1.

Second, consider high ($\omega \gg \omega_p$) frequencies. Each passing electron induces on one sphere the potential $V(t) = e/(4\pi\epsilon_0 r(t))$ with $r^2 = p^2 + v_T^2 t^2$. If $p < v_T/\omega$, this is a pulse of amplitude $e/(4\pi\epsilon_0 p)$ and width p/v_T. Taking the power spectrum and summing over the event rate $\approx \pi (v_T/\omega)^2 n v_T$ yields nearly the ω^{-2} spectrum given in Table 1. (Since $\omega \gg \omega_p$, $v_T/\omega \ll L$, so that the noise on the dipole is just twice that on one sphere.) This assumes implicitly that the sphere radius satisfies $a < v_T/\omega$. Otherwise, there remains only the (smaller) contribution from electrons passing at $p > v_T/\omega$, yielding a generic ω^{-4} spectrum in the limiting case $\omega a/v_T \gg 1$.

A key point is that for $\omega < \omega_p$ we see electrons up to the distance L_D, while for $\omega \gg \omega_p$ we mostly see them up to v_T/ω.

Now, what happens for $\omega \approx \omega_p$? Since our antenna detects mostly the plasma waves satisfying $k_p \geq 1/L$, we expect a noise peak just above the plasma frequency, at a distance of the order of $\delta\omega/\omega_p \approx (L_D/L)^2$ (the exact figure is somewhat larger; a better approximation is given in Table 1). We insist on this point because this distance has sometimes been interpreted as a Doppler shift [see *Harvey et al.*, 1979]. Note that since both the wave number and the inverse of the damping length tend to zero at ω_p, the antenna now senses a very large plasma volume.

How are those results modified if we use a wire dipole instead of small spheres?

The critical parameter is the value of kL: the relevant scales are $k_0 \approx 1/L_D$ for $\omega < \omega_p$, $k_0 \approx k_p$ for $\omega \approx \omega_p$, and $k_0 \approx \omega/v_T$ for $\omega \gg \omega_p$. Thus, except at the noise peak $\omega \approx \omega_p$, one has $k_0 L \gg 1$, and the noise will be $k_0 L$ times smaller than for the spheres. This gives approximately the results of Table 1.

2.4 *On Being Small*

Take a short antenna, namely $L < L_D$: it favours $k \approx 1/L > 1/L_D$ (for the wire) or $k \geq 1/L > 1/L_D$ (for the sphere). We know that for $kL_D \geq 1$, the plasma temporal dispersion is small. Thus, we expect a nearly white spectrum even if $\omega > \omega_p$: for one sphere, the amplitude is the same as calculated in section 2.3 for $\omega < \omega_p$. But now the two spheres see correlated signals: since the correlation scale $\approx L_D$, the noise spectrum measured between the two spheres is $(L/L_D)^2$ times that on one sphere.

Since we now have $kL \ll 1$, this result also holds for a wire dipole, and we get approximately all the results of Table 2.

3 THEORETICAL TOOLS

3.1 *Antenna Geometry*

The important quantity is the current distribution on the antenna. We consider below the two main configurations used in space experiments (Figure 1).

3.1.1 Wire dipole antenna. It consists of two cylinders, each of length L and radius $a \ll L$, parallel to the **Oz** axis, separated by an infinitesimal gap. The current distribution $\mathbf{J}(\mathbf{r})$ is generally difficult to calculate, and we assume that it has a linear form (namely the charge distribution is constant on each arm). This approximation has a rather wide range of validity whenever $\omega L/c \ll 1$ and $a/L_D \ll 1$. Whence, in Fourier space,

$$\mathbf{J}(\mathbf{k}) = \int d\mathbf{r}\mathbf{J}(\mathbf{r})e^{-i\mathbf{kr}} \tag{1}$$

$$\mathbf{J}(\mathbf{k}) = \frac{4}{k_z^2 L}\sin^2(k_z L/2)\left[J_0(k_r a)\right]\mathbf{e_z} \tag{2}$$

where $k^2 = k_z^2 + k_r^2$, and J_0 is the zero-order Bessel function of the first kind.

3.1.2 Double-sphere antenna. It consists of two spheres of radius a, separated by $L \gg a$ along the **Oz** axis. Then

$$\mathbf{J}(\mathbf{k}) = -\frac{2i}{k_z}\sin(k_z L/2)\left[\frac{\sin(ka)}{ka}\right]\mathbf{e_z} \tag{3}$$

In general, the radius satisfies $ka \ll 1$ for the relevant values of k, and the quantities in brackets in (2) and (3) can be replaced by 1. (This is not true for calculating the capacitance, since it involves the field at a distance $r \approx a$.)

3.2 *Voltage Spectral Density*

Let the antenna be immersed in a fluctuating electric field defined by the spectral distribution of its correlation tensor (see, for instance, *Sitenko* [1967])

$$E_{ij}(\mathbf{k},\omega) = \int_{-\infty}^{+\infty} dt \int \mathbf{dr} E_{ij}(\mathbf{r},t)\, e^{i(\omega t - \mathbf{k}.\mathbf{r})} \quad (4)$$

$$E_{ij}(\mathbf{r},t) = \langle E_i(\mathbf{r}_1,t_1)\, E_j(\mathbf{r}_1+\mathbf{r},t_1+t)\rangle \quad (5)$$

The voltage spectral density at the antenna terminals is

$$V^2 = 2\int_{-\infty}^{+\infty} dt \langle V(t_1)\, V(t_1+t)\rangle\, e^{i\omega t} \quad (6)$$

$$= \frac{2}{(2\pi)^3}\int \mathbf{dk} J_i(\mathbf{k})\, E_{ij}(\mathbf{k},\omega)\, J_j^*(\mathbf{k}) \quad (7)$$

(the usual convention of positive frequencies is implied, and V^2 is in $\mathrm{V^2 Hz^{-1}}$).

In general, the terminals of the antenna (of impedance Z) are connected to a receiver with a finite input impedance Z_R. The spectral density at the receiver input terminals is then

$$V_R^2 = V^2 |Z_R/(Z_R+Z)|^2 \quad (8)$$

3.3 *The Antenna Impedance*

The antenna impedance is

$$Z = \frac{i}{(2\pi)^3 \epsilon_0 \omega}\int \mathbf{dk} J_i(\mathbf{k}) \Lambda_{ij}^{-1}(\mathbf{k},\omega)\, J_j(\mathbf{k}) \quad (9)$$

$$\Lambda_{ij}(\mathbf{k},\omega) = \frac{k^2c^2}{\omega^2}\left(\frac{k_i k_j}{k^2} - \delta_{ij}\right) + \epsilon_{ij}(\mathbf{k},\omega) \quad (10)$$

For ω of the order of magnitude of ω_p, one can approximate the field as deriving from a scalar potential (if $\omega \ll kc$). Then, (9) simplifies to

$$Z = \frac{i}{(2\pi)^3 \epsilon_0 \omega}\int \mathbf{dk} \frac{|\mathbf{k}.\mathbf{J}(\mathbf{k})|^2}{k^2 \epsilon_L} \quad (11)$$

$\epsilon_L = \epsilon_L(\mathbf{k},\omega) = k_i.\epsilon_{ij}.k_j$ being the plasma longitudinal permittivity.

If the plasma is in thermal equilibrium at temperature T, the formulae reduce to

$$V^2 = 4KT \ \mathrm{Re}(Z) \quad (12)$$

where K is Boltzmann's constant and Re denotes the real part.

3.4 *Particle Impacts or Emission*

The above expressions assume a "grid antenna" in a homogeneous plasma; namely, we have neglected the fact that the antenna is a physical object which disturbs the trajectories of the particles since they cannot pass through its surface: it collects electrons and ions and may also emit photoelectrons and/or secondary particles.

In general, the problem becomes very complicated [see *Calder and Laframboise*, 1985]. Fortunately, in space plasmas, the antenna radius a and dc potential ϕ often satisfy $a < L_D$ and $|e\phi/KT| < 1$. Then, a good approximation for the total noise at the antenna terminals below the plasma frequency can be obtained [*Meyer-Vernet*, 1983*a*] by simply adding to (7) the term

$$V_I^2 = \sum_s q_s^2 N_s |Z|^2 \quad (13)$$

where the summation extends over all the processes exchanging a charge q_s at a mean rate N_s per second with each antenna arm. If the charging processes are impacts of electrons and ions and photoelectron emission, (13) simplifies to (owing to the current balance)

$$V_I^2 = 2e^2 N_e |Z|^2 \quad (14)$$

where N_e is the plasma electron impact rate on the surface of one antenna arm.

4 MAXWELLIAN ELECTRONS

Although most space plasmas are neither in equilibrium nor isotropic, the isotropic Maxwellian model often yields a rather good approximation of the noise (and a still better approximation of the impedance) at frequencies of the order of magnitude of the plasma frequency.

4.1 *Impedance and Thermal Noise*

Equation (11) reduces to

$$Z = \frac{4i}{\pi^2 \epsilon_0 \omega}\int_0^\infty dk \frac{F(k)}{\epsilon_L} \quad (15)$$

$$F(k) = (1/32\pi)\int d\Omega\, |\mathbf{k}.\mathbf{J}(\mathbf{k})|^2 \quad (16)$$

where in (16) the integration is over the direction of $\mathbf{k}$ ($d\Omega = \sin\theta d\theta d\phi$), so that we have from (2) and (3), for the two geometries,

Wire dipole

$$F(k) = F_1(kL)\left[J_0^2(ka)\right] \quad (17)$$

$$F_1(x) = \left[\mathrm{Si}(x) - \mathrm{Si}(2x)/2 - 2\sin^4(x/2)/x\right]/x \quad (18)$$

(Si denotes the sine integral function.)

Sphere dipole

$$F(k) = \frac{1}{4}\left(1 - \frac{\sin(kL)}{kL}\right)\left[\frac{\sin^2(ka)}{k^2a^2}\right] \quad (19)$$

If $ka \ll 1$, one gets, for the two respective dipoles,

Wire or sphere, for $kL \ll 1$

$$F(k) \approx k^2L^2/24$$

Wire, for $kL \gg 1$

$$F(k) \approx \pi/(4kL)$$

Sphere, for $kL \gg 1$

$$F(k) \approx 1/4$$

Note that (in agreement with section 2.1) $F(k)$ has a broad peak at $kL \approx 3{\cdot}5$ for the wire dipole [see *Kuehl*, 1966], while for the spheres it is independent of kL when $kL \gg 1$.

The permittivity is given by

$$\epsilon_L(k,\omega) = 1 + \left[1 - \Phi(z) + i\pi^{1/2} z e^{-z^2}\right]/k^2 L_D^2 \quad (20)$$

$$\Phi(z) = 2ze^{-z^2}\int_0^z dx e^{x^2} \quad (21)$$

In (20), $v_T = (2KT/m)^{1/2}$, $\omega_p = 2\pi f_p = \left(ne^2/\epsilon_0 m\right)^{1/2}$, where n and T are the electron density and temperature, $L_D = v_T/2^{1/2}\omega_p$, and $z = \omega/kv_T$; we have neglected the ion contribution (see section 6.2).

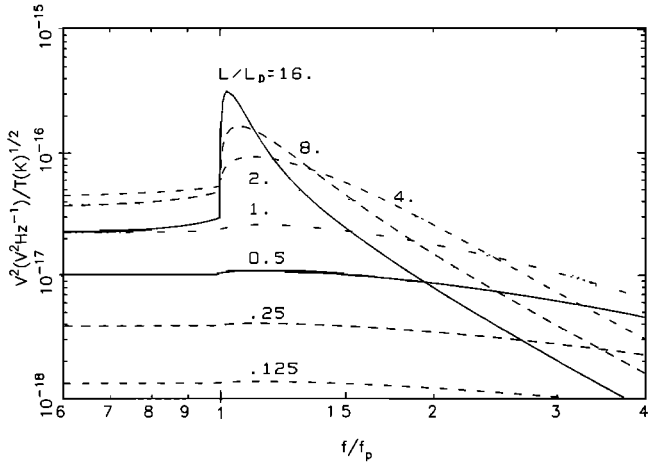

Fig. 2. Normalized thermal noise spectra $V^2(\mathrm{V^2Hz^{-1}})/T^{1/2}$ (K) as a function of f/f_p, for a wire dipole antenna with different values of L/L_D. For $L/L_D \gg 1$, the high-frequency spectra vary as f^{-3}. For $L/L_D < 1$, the spectra are nearly flat.

The thermal noise is then obtained from (8), (12), and (15).

4.1.1 Numerical results. A few numerical results for a wire dipole can be found in the work by *Kuehl* [1967] (infinitesimal radius) and *Couturier et al.* [1981]. The quantity $ZT^{1/2}$ depends only on f/f_p, L/L_D, and a/L_D; if $a/L_D \ll 1$, then $V^2/T^{1/2}$ depends only on f/f_p and L/L_D.

Figures 2 and 3 show a grid of normalized spectra for the wire dipole and the double-sphere antenna, respectively. Figures 4 and 5 show the spectrum level below f_p (where it is nearly flat) as a function of the electron density and temperature.

4.1.2 Analytical results. Analytical results can be obtained in several limiting cases [*Balmain*, 1965; *Kuehl*, 1966; *Schiff*, 1970; *Schiff and Fejer*, 1970; *Meyer-Vernet*, 1979, 1983*a*].

First, if $L \gg L_D$, the main contribution to the integral (15) stems from $kL_D \ll 1$, and one can use the hydrodynamic approximation of ϵ_L (which is equivalent to developing Φ up to second order in $1/z^2$ in (20) for $\omega \approx \omega_p$), i.e.,

$$\epsilon_L(k,\omega) \approx 1 - \frac{\omega_p^2}{\omega^2 - 3k^2v_T^2/2 + i\sigma} \qquad (22)$$

where $i\sigma$ denotes an infinitesimal positive imaginary part. Then, one integrates (15) by residues, whence the real part

$$\mathrm{Re}(Z) = 2F(k_p)/\left(3\pi\epsilon_0\omega L_D^2 k_p\right) \qquad (23)$$

with $k_p = \left(\omega^2/\omega_p^2 - 1\right)^{1/2}/3^{1/2}L_D$, and $F(k)$ defined in (17) and (19). In particular, the corresponding amplitude and frequency of the noise peak are deduced from the maximum of the function $F(k)/k$ (see Table 1).

This does not give $\mathrm{Re}(Z)$ whenever $f < f_p$, since the pole k_p is then nearly imaginary. Then, one returns to (20) and develops the real part for $z \ll 1$, i.e.,

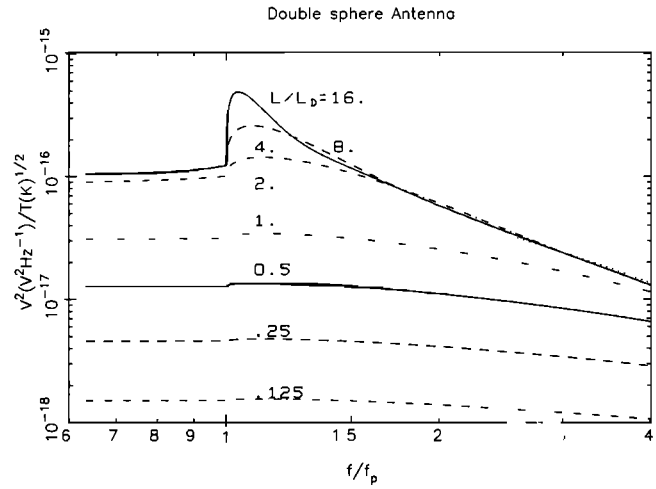

Fig. 3. Same as Figure 2, for a double-sphere antenna. For $L/L_D \gg 1$, the high-frequency level varies as f^{-2} and does not depend on L. If $L/L_D \ll 1$, the level is the same as for the wire dipole. See section 4.2 before using this figure.

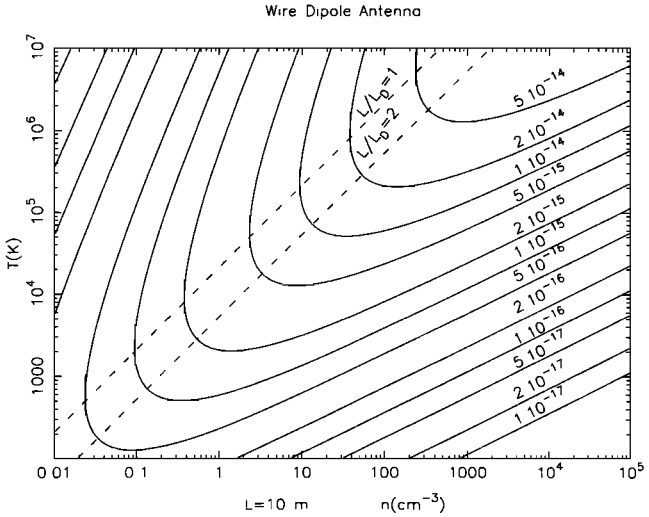

Fig. 4. Thermal noise level (V^2 in $\mathrm{V^2Hz^{-1}}$) for $f/f_p = 0.5$ where the spectrum is nearly flat, as a function of the plasma density and temperature, for a thin wire dipole antenna with $L = 10$ m. Since the density scales as L^{-2}, one can use this chart with any antenna length: for instance if $L = 50$ m, then the density n on this figure must be divided by 25. The dashed lines correspond to the plasma parameters for which $L/L_D = 1$ and 2: for $L/L_D \approx 1$, the diagnosis of T is not accurate.

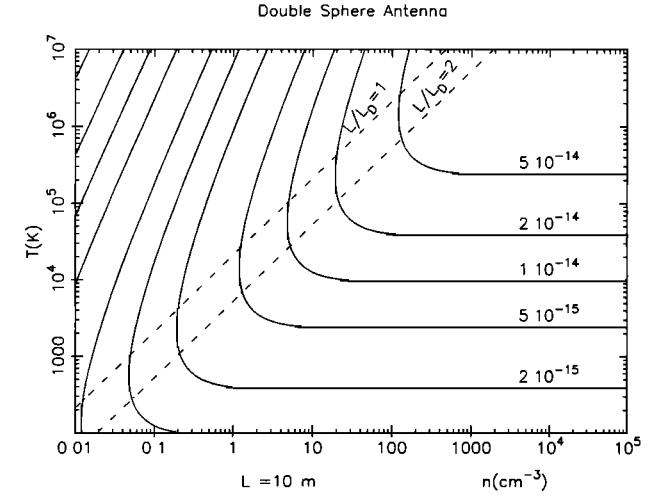

Fig. 5. Same as Figure 4, for a double-sphere antenna.

TABLE 1. Impedance $Z = R + iI$ (in ohms) and noise V^2 (in $V^2 Hz^{-1}$) for a long dipole ($a \ll L_D \ll L$) in a thermal plasma; $x = f/f_p$

WIRE DIPOLE

$V_0^2 = \pi^{1/2} m v_T L_D/(2\epsilon_0 L) = 5 \times 10^{-16} T^{1/2} L_D/L$

$R_0 = 9 \times 10^6\ T^{-1/2}\ L_D/L$

$I = \ln(L_D/a)/(\pi\epsilon_0\omega L)$ for $x \ll 1$

$I = [\ln(L/a) - 1]/(\pi\epsilon_0\omega L)$ for $x \gg 1$

peak: $x \approx 1 + 8(L_D/L)^2$ $V^2 \approx 0{\cdot}04\ V_0^2\,(L/L_D)^2$

	$x < 1$	$1 + (5L_D/L)^2 < x < (L_D/a)^2$
$V^2/V_0^2 = R/R_0$	1	$1{\cdot}6/\left[x\left(x^2 - 1\right)\right]$

DOUBLE-SPHERE

$V_0^2 = m\ v_T/\left(\pi^{3/2}\epsilon_0\right) = 10^{-16}\ T^{1/2}$

$R_0 = 1{\cdot}8 \times 10^6\ T^{-1/2}$ $I = 1/(2\pi\epsilon_0\omega a)$

peak: $x \approx 1 + 15(L_D/L)^2$ $V^2 \approx 0{\cdot}27\ V_0^2 L/L_D$

	$x < 1$	$1 \ll x < (L_D/a)^2$
$V^2/V_0^2 = R/R_0$	1	$2/x^2$

Error < 30% for $L \geq 7L_D$. Notation defined in section 4.1 ; SI units.

$$\mathrm{Re}(\epsilon_L) \approx 1 + 1/k^2 L_D^2 \qquad (24)$$

If $L \ll L_D$, one uses (24), and the value of F for $kL \ll 1$.

Tables 1 and 2 give the results and their ranges of validity for the two antenna geometries.

4.2 *Particle Impacts or Emission*

How are those results changed by the particle impacts or emission? If the antenna dc potential ϕ and radius a satisfy $|e\phi/KT| < 1$ and $a < L_D$, then the electron impact rate on one antenna arm is approximately

TABLE 2. Impedance $Z = R + iI$ and noise V^2 for a short (wire or double-sphere) dipole ($a \ll L \ll L_D$) in a thermal plasma. $x = f/f_p$

$V_0^2 = m v_T L^2/\left(3\pi^{3/2}\epsilon_0 L_D^2\right) = 3{\cdot}4 \times 10^{-17} T^{1/2}\,(L/L_D)^2$

$R_0 = 6.2 \times 10^5\ T^{-1/2}\,(L/L_D)^2$

$I = [\ln(L/a) - 1]/(\pi\epsilon_0\omega L)$ for WIRE DIPOLE

$I = 1/(2\pi\epsilon_0\omega a)$ for DOUBLE-SPHERE

	$x < 1$	$1 < x < 1{\cdot}5\ L_D/L$
$V^2/V_0^2 = R/R_0$	$1 + \ln(L_D/L)$	$1 + \ln\left[2^{1/2}\ L_D/(xL)\right]$

Error < 30% for $L < L_D/4$. Notation defined in section 4.1.

TABLE 3. Noise V_I^2 due to impacts and photoemission in a thermal plasma. $x = f/f_p \ll 1$

WIRE DIPOLE

$V_{0I}^2 = 2\ m\ v_T a/\left(\pi^{3/2}\epsilon_0 L x^2\right) = 2.\ 10^{-16} T^{1/2} a/\left(L x^2\right)$

	$L/L_D \ll 1$	$L/L_D \gg 1$
V_I^2/V_{0I}^2	$[\ln(L/a) - 1]^2$	$[\ln(L_D/a)]^2$

DOUBLE-SPHERE

$V_I^2 = m v_T/\left(\pi^{3/2}\epsilon_0 x^2\right) = 10^{-16} T^{1/2}/x^2$

Notation defined in section 4.1.

$$N_e = (4\pi)^{-1/2}\, n v_T S \qquad (25)$$

with $S = 2\pi a L$ (wire) or $S = 4\pi a^2$ (sphere).

The corresponding spectrum to be added to the results of section 3.1 is obtained by inserting (25) in (14) and is given in Table 3. It is important to note that the relative contribution of this noise, V_I^2/V^2 for $x = f/f_p < 1$ is given by

Wire

$4a[\ln(L_D/a)]^2 / \left[\pi^2 L_D x^2\right]$ $L \gg L_D$

$6aL_D^2[\ln(L/a)]^2 / \left[L^3 x^2 \ln(L_D/L)\right]$ $L \ll L_D$

Sphere

$1/x^2$ $L \gg L_D$

$L_D^2/\left[L^2 x^2 \ln(L_D/L)\right]$ $L \ll L_D$

Thus, though generally negligible for the wire dipole, it is dominant for the double-sphere antenna.

Two remarks are in order. First, this absorption or emission of particles also changes the antenna impedance (broadly speaking, it adds in parallel to Z a resistance $R \approx (e\ dN_e/d\phi)^{-1}$); in practice this does not significantly change $|Z|$ for frequencies of the order of magnitude of f_p if $|e\phi/kT| < 1$. Second, the condition $|e\phi/KT| < 1$ may not hold, especially when the photoelectron emission is small: then N_e becomes $N_e A$ where $A = \exp(e\phi/KT)$ if $\phi < 0$ and $A = (1 + e\phi/KT)^n$ if $\phi > 0$, with $n = 1/2$ and $n = 1$ for the wire and the sphere, respectively [see *Laframboise and Parker*, 1973].

4.3 *Quick Diagnosis*

In general, a precise plasma diagnosis by thermal noise spectroscopy requires a fitting of the measured spectrum V_R^2, using (8), (15), and (12). However, with a wire antenna satisfying $L \gg L_D$ one can perform a quick approximate diagnosis:

1. Deduce the plasma frequency f_p from the spectrum cutoff.

2. Obtain an approximation of the antenna impedance Z (from Tables 1 and 2), and deduce the spectrum level V^2 at the antenna terminals from (8).

3. Deduce the temperature T from the level V^2 below f_p

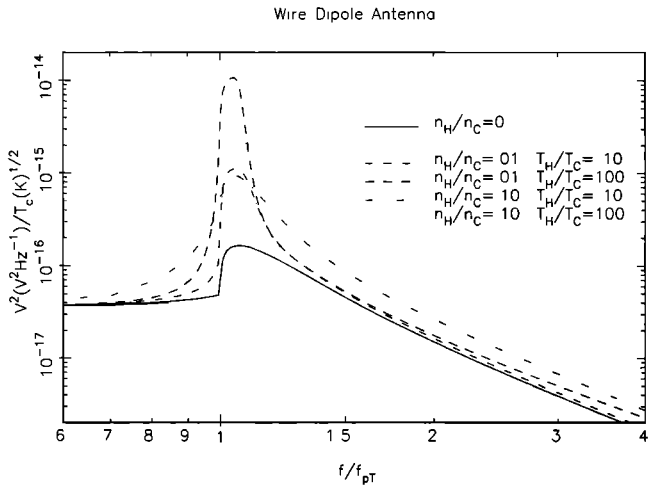

Fig. 6. Normalized quasi-thermal noise spectra V^2 (V^2Hz^{-1}) $/T^{1/2}$ (K) as a function of f/f_{pT} for a wire dipole antenna with $L/L_{DC} = 8$, and different values of hot electron parameters. The main effect of adding hot electrons is to multiply the peak level by T_H/T_C; the low-frequency level is nearly independent of the hot electrons, while the high-frequency level is proportional to the total electron pressure ($\propto n_C T_C + n_H T_H$).

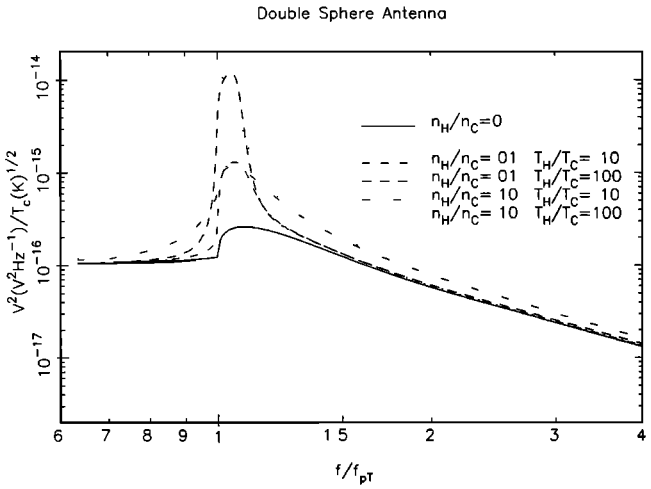

Fig. 7. Same as Figure 6, for a double-sphere antenna with $L/L_{DC} = 8$. The same remarks hold, but the high-frequency level is now proportional to the total electron flux ($\propto n_C T_C^{1/2} + n_H T_H^{1/2}$).

(where it is nearly flat) by using Figure 4 or Table 1. Note that if $L \approx L_D$, the method does not work well since the peak is not well defined and the temperature determination from the low-frequency level is not unique.

5 TWO MAXWELLIAN ELECTRON POPULATIONS

How are the above results changed if the plasma is not Maxwellian? Let us consider two Maxwellian electron populations. The impedance is still given by (15), but now

$$\epsilon_L(k,\omega) = 1 + \sum_{P=C,H} \frac{1 - \Phi(z_P) + i\pi^{1/2} z_P e^{-z_P^2}}{k^2 L_{DP}^2} \quad (26)$$

where n_C, T_C, n_H, T_H are the density and temperature of respectively the cold (C) and hot (H) components and $z_P = \omega/(kv_{TP})$, $v_{TP} = (2KT_P/m)^{1/2}$, and $L_{DP} = \left(\epsilon_0 KT_P/\left(n_P e^2\right)\right)^{1/2}$, with $P = C, H$.

The voltage spectral density at the antenna terminals is

$$V^2 = \frac{16K}{\pi^{3/2}\epsilon_0\omega} \int_0^\infty dk \frac{F(k)}{|\epsilon_L|^2} \sum_{P=C,H} \frac{T_P z_P}{k^2 L_{DP}^2} e^{-z_P^2} \quad (27)$$

A few results are given by *Meyer-Vernet* [1979] and *Couturier et al.* [1981] for the wire dipole antenna. We include here the double-sphere antenna.

5.1 Antenna Impedance and Quasi-Thermal Noise

5.1.1 Numerical results. By comparing (12), (15), and (27), one sees that the noise is much more modified by the presence of the hot population than is the impedance. Figures 6 to 9 show some examples of spectra in both geometries.

Broadly speaking, the introduction of a hot population with $\alpha = n_H/n_C < 1$, $t = T_H/T_C > 1$, has the following consequences:

1. If $f \ll f_{pT}$ ($f_{pT} = f_{pC}(1+\alpha)^{1/2}$ being the total plasma frequency and f_{pC} the cold one), the noise is negligibly modified provided $\alpha t^{-1/2} \ll 1$ for the long wire, and a still weaker condition otherwise.
2. The cut-off is no longer abrupt and occurs at f_{pT}.
3. If $L \gg L_D$, the peak level near f_{pT} is increased by the factor t; otherwise, it is much less modified.
4. For $f \gg f_{pT}$, the noise is multiplied by $(1+\alpha t)$ for the long wire and more weakly modified otherwise.

5.1.2 Analytical results. Analytical results are obtained by developing F and Φ for large and/or small arguments. The pole of ϵ_L is now

$$k_b \approx \frac{1+\alpha}{L_{DC}} \left[\frac{1 - \omega_{pT}^2/\omega^2}{3(1+\alpha t)}\right]^{1/2}$$

where $\omega \approx \omega_{pT}$, and its contribution to the resistance, which is dominant when $L \gg L_{DC}$, becomes instead of (23)

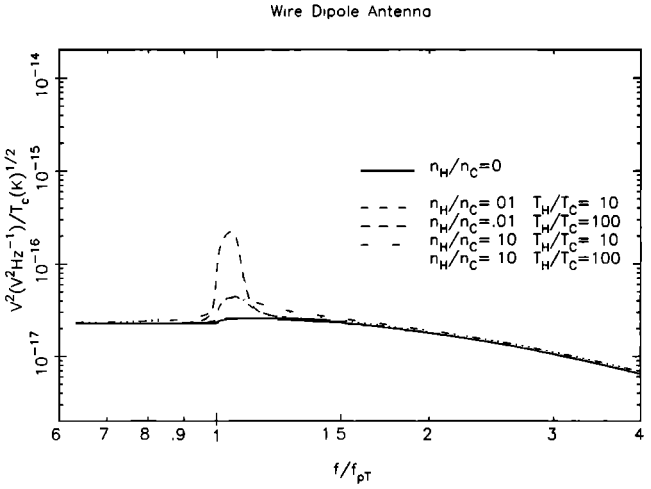

Fig. 8. Normalized quasi-thermal noise spectra $V^2(V^2Hz^{-1})/T^{1/2}$ (K) as a function of f/f_{pT} for a wire dipole antenna with $L/L_{DC} = 1$ and different values of hot electron parameters. Note that the level is now much less sensitive to the hot electron parameters.

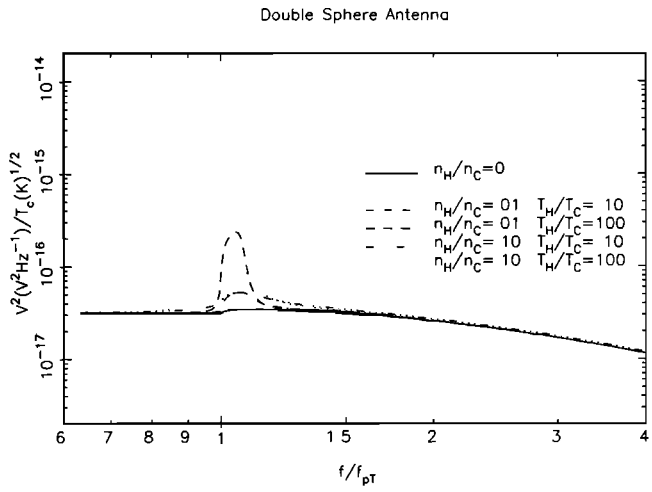

Fig. 9. Same as Figure 8, for a double-sphere antenna with $L/L_{DC} = 1$.

$$\mathrm{Re}(Z) = \frac{2F(k_b)(1+\alpha)^2}{3\pi\epsilon_0\omega L_{DC}^2 k_b(1+\alpha t)} \qquad (28)$$

(F is defined in section 4.1). The contribution to the noise is

$$V^2 = 4KT_C\mathrm{Re}(Z)\frac{1+C\alpha t^{-1/2}}{1+C\alpha t^{-3/2}} \qquad (29)$$

with $C = \exp\left[\omega^2(1-1/t)/(k_b v_{TC})^2\right]$. Thus, although the resistance is barely modified, the noise peak amplitude increases by the factor t. Note that (28) and (29) are correct approximations for the resistance and the noise peak just above f_{pT} only when $L \gg L_{DC}$; otherwise the pole contribution is not necessarily dominant.

Other analytical expressions are given in Tables 4, 5 , and 6.

TABLE 4. Impedance $Z = R + iI$ and noise V^2 for a long wire dipole ($a \ll L_D \ll L$) with two Maxwellian electron populations. $x = f/f_{pT}$

WIRE DIPOLE

$V_0^2 = 5 \times 10^{-16}\, T_C^{1/2} L_{DC}/L$

$R_0 = 9 \times 10^6\, T_C^{-1/2}\, L_{DC}/L$

$I = \ln(L_{DC}/a)/(\pi\epsilon_0\omega L)$ for $x \ll 1$

$I = [\ln(L/a) - 1]/(\pi\epsilon_0\omega L)$ for $x \gg 1$

peak: $x \approx 1 + 8(L_{DC}/L)^2(1+\alpha t)/(1+\alpha)^2$
$V^2 \approx 0{\cdot}04\, t\, V_0^2 (L/L_{DC})^2 (1+\alpha)^{3/2}/(1+\alpha t)$

	$x \ll 1$	$t^{1/2} < x < (L_D/a)^2$
V^2/V_0^2	$(1+\alpha t^{-1/2}) \times (1+\alpha/t)^{-3/2}$	$1{\cdot}6(1+\alpha t) \times x^{-3}(1+\alpha)^{-3/2}$
R/R_0	$(1+\alpha t^{-3/2}) \times (1+\alpha/t)^{-3/2}$	$1{\cdot}6(1+\alpha) \times x^{-3}(1+\alpha)^{-3/2}$

Notation defined in section 5. We have neglected small terms in the logarithms in order to avoid too complicated expressions.

TABLE 5. Impedance $Z = R + iI$ and noise V^2 for a long double-sphere dipole ($a \ll L_{DC} \ll L$) with two Maxwellian electron populations. $x = f/f_{pT}$

DOUBLE-SPHERE

$V_0^2 = mv_{TC}/(\pi^{3/2}\epsilon_0) = 10^{-16}\, T_C^{1/2}$

$R_0 = 1{\cdot}8 \times 10^6\, T_C^{-1/2}$ $\qquad I = 1/(2\pi\epsilon_0\omega a)$

peak: $x \approx 1 + 15(L_{DC}/L)^2(1+\alpha t)/(1+\alpha)^2$
$V^2 \approx 0{\cdot}27\, t\, V_0^2 (L/L_{DC})(1+\alpha)^{3/2}/(1+\alpha t)$

	$x \ll 1$	$t^{1/2} < x < (L_D/a)^2$
V^2/V_0^2	$(1+\alpha t^{-1/2}) \times (1+\alpha/t)^{-1}$	$1{\cdot}45(1+\alpha t^{1/2}) \times x^{-2}(1+\alpha)^{-1}$
R/R_0	$(1+\alpha t^{-3/2}) \times (1+\alpha/t)^{-1}$	$1{\cdot}45(1+\alpha t^{-1/2}) \times x^{-2}(1+\alpha)^{-1}$

Notation defined in section 5.

5.2 *Particle Impacts or Emission*

With two Maxwellian electron populations, the electron impact rate trivially becomes

$$N_e \approx (4\pi)^{-1/2} n_C v_{TC}\left(1+\alpha t^{1/2}\right) S \qquad (30)$$

The corresponding spectrum to be added to the results of section 5.1 is approximately (neglecting small changes in logarithmic terms) that given in Table 3 multiplied by the

TABLE 6. Impedance $Z = R + iI$ and noise V^2 for a short dipole ($a \ll L \ll L_{DC}$) with two Maxwellian electron populations. $x = f/f_{pT}$

$V_0^2 = 3{\cdot}4 \times 10^{-17}\, T^{1/2}(L/L_{DC})^2$

$R_0 = 6.2 \times 10^5\, T^{-1/2}\, (L/L_{DC})^2$

$I = [\ln(L/a) - 1]/(\pi\epsilon_0\omega L)$ for WIRE DIPOLE

$I = 1/(2\pi\epsilon_0\omega a)$ for DOUBLE-SPHERE

	$x < 1$	$1 < x < 1{\cdot}5\, L_{DC}/L$
$\frac{V^2}{V_0^2}$	$(1+\alpha t^{-1/2}) \times [1+\ln(L_{DC}/L)]$	$(1+\alpha t^{-1/2}) \times \left[1+\ln\left(2^{1/2}L_{DC}/(Lx)\right)\right]$
$\frac{R}{R_0}$	$(1+\alpha t^{-3/2}) \times [1+\ln(L_{DC}/L)]$	$(1+\alpha t^{-3/2}) \times \left[1+\ln\left(2^{1/2}L_{DC}/(Lx)\right)\right]$

Notation defined in section 5. We have neglected small terms in the logarithms in order to avoid too complicated expressions. The formula for V^2/V_0^2 in the column $x > 1$ holds only when $x > 1 + 1/\ln\left(t^{3/2}/\alpha\right)$.

factor $\left(1+\alpha t^{1/2}\right)$. It is still generally negligible for the wire dipole and dominant for the double-sphere antenna.

5.3 *Plasma Diagnosis Guide*

What are the consequences for the diagnosis of two Maxwellian (n_C,T_C,n_H,T_H) electron populations by thermal noise spectroscopy?

The best antenna is the $L \gg L_D$ wire dipole, since the impact noise is negligible and the quasi-thermal noise peak is well defined. Although a precise diagnosis should involve numerical computations from (8), (15), (26), and (27), a partial diagnosis can still be quickly performed if the hot population satisfies $\alpha = n_H/n_C \ll 1$:

1. Calculate V^2 from the measured spectrum V_R^2 by using (8) and approximations of Z.
2. Deduce the total density from the spectrum cutoff which occurs at f_{pT}.
3. Deduce T_C from the flat spectrum level below f_{pT} by using Table 1 or Figure 4.
4. Then, the high-frequency level (where V^2 varies as f^{-3}) yields the total electron pressure; the final step (deducing separately n_H and T_H) requires a fitting of the peak shape, for which analytical results only provide an order of magnitude estimation.

6 WHY DOES IT WORK?

Are the above results relevant for the average space experiment, which often involves queer antennae in complicated plasmas?

In a surprising number of cases, the answer is "yes."

6.1 *Real antennae*

The actual antenna must be sufficiently close to the theoretical model. This is rather easy to achieve for a linear wire dipole: one must only ensure that it be larger than the Debye length and the spacecraft size (or located sufficiently far from it, in order to be outside the spacecraft plasma sheath).

The case of the double-sphere antenna is less clean, since the spheres must be mounted on booms, which intrinsically modify the problem (the equipotentials are modified, and the function $F(k)$ is no longer given by (19) except for $kL \ll 1$). This is an additional argument to reject this antenna for thermal noise spectroscopy or for longitudinal field measurements.

Yet, queer antenna geometries are often imposed by spacecraft designers. What happens in this case?

We consider below two common examples: a wire linear dipole with a large gap between its arms, and a wire dipole with an angle of $\pi/2$ between its arms; the latter case corresponds to the Voyager spacecraft configuration.

6.1.1 Linear wire dipole with a gap. Take two thin ($a \ll [L, L_D]$) wires, each of length L, with a gap of size $2d$ along the **Oz** axis and a linear current distribution. Then, (2) and (17) are replaced by

$$\mathbf{J}(\mathbf{k}) = \frac{4}{k_z^2 L}\sin(k_z L/2)\sin(k_z(d+L/2))\,\mathbf{e_z} \qquad (31)$$

$$F(k) = \{f[k(L+2d)] + f(kL) - f[2k(L+d)]/2 - f(2kd)/2 - [\cos(k(L+d)) - \cos(kd)]^2\} / \left(2k^2L^2\right) \qquad (32)$$

where $f(x) = x\mathrm{Si}(x)$. Of course, (32) reduces to (17) (wire dipole with infinitesimal gap) in the limit $d \to 0$, and to (19) (double sphere) in the limit $L \to 0$.

The consequences are straightforward for small or large dipoles. If $kL \ll 1$ and $kd \ll 1$, then $F(k) \approx k^2(L+2d)^2/24$, and the effect of the gap is to replace L by $L+2d$. But if $kL \gg 1$ and $kd \gg 1$, then $F(k) \approx \pi/(4kL)$, and the antenna behaves as if the gap were infinitesimal. Note, however, that those results do not apply if there is a spacecraft inside the gap.

6.1.2 V-shaped wire dipole. We take two thin wires, each of length L, aligned with the **Ox** and **Oy** axis, respectively, with an infinitesimal gap, and a linear current distribution. Then

$$\mathbf{J}(\mathbf{k}) = G(k_x)\,\mathbf{e_x} - G(k_y)\,\mathbf{e_y} \qquad (33)$$

$$G(x) = \frac{1}{ix} - \frac{e^{-ixL}-1}{x^2 L} \qquad (34)$$

The general expression of the function $F(k)$ obtained from (16) is awful, but it simplifies to

If $kL \ll 1$

$$F(k) \approx k^2L^2/48$$

If $kL \gg 1$

$$F(k) \approx \pi/(4kL)$$

Comparing to section 4.1, we deduce that a short V-shaped dipole behaves as a linear dipole of half-length $L/2^{1/2} = L\cos\pi/4$ (i.e. the antenna projection on a plane perpendicular to its symmetry axis), but a long V dipole behaves as if its arms were colinear.

Consequently, for a long wire antenna ($L \gg L_D$), such complications as a finite gap or a noncolinearity between the arms do not change very much the noise spectrum provided that $|f-f_p|/f_p$ is much larger than a few $(L_D/L)^2$. This fact is contrary to the intuition acquired with short antennae, but not surprising: if the mean distance between the arms is large, then they "see" uncorrelated signals (except for $f \approx f_p$), and the noise detected by the dipole is twice that on one arm, whatever their relative location.

6.2 *In Real Plasmas*

Are actual geophysical plasmas as simple as we have assumed? Certainly not.

In particular, the electron velocity distribution is seldom made of two Maxwellian functions, the ions are not static, and there is often a drift velocity between the antenna and the plasma, and a static magnetic field.

We discuss below some of these effects.

6.2.1 Ions. In the previous sections, we have neglected the ion motion. Is this correct?

Let us consider a thermal plasma in the antenna frame. We can neglect the ion motion if their thermal velocity satisfies $v_{Ti} \ll \omega/k$, namely if $\omega L/v_{Ti} \gg 1$. For ω of the order of ω_p, this condition requires $L/L_D \gg (m/M)^{1/2}$ where M is the ion mass. On the other hand, if $\omega L/v_{Ti} \leq 1$, the ion contribution to the thermal noise amounts approximately to multiplying by $(M/m)^{1/2}$ (≈ 43 for H+ ions) the R and V^2 expressions given in Table 2 [*Meyer-Vernet*, 1983*b*].

6.2.2 Drift velocity. What happens if there is a drift velocity **v** between the plasma and the antenna?

The system is not in equilibrium, so that (12) no longer

holds. For calculating the impedance and the noise, one must use the plasma quantities in the antenna frame, i.e., $\Lambda^{-1}(k, \omega - \mathbf{k}.\mathbf{v})$ in (9) and $E_{ij}(k, \omega - \mathbf{k}.\mathbf{v})$ in (7), respectively. In this case, the ion contribution becomes important if the condition $(\omega - \mathbf{k}.\mathbf{v})/kv_{Ti} \gg 1$ does not hold, and, as is well known [see *Ginzburg*, 1979; *Fiala*, 1970], one gets negative resistances (and possibly noise amplification) if the range of k satisfying $\omega - \mathbf{k}.\mathbf{v} < 0$ dominates the integral in (9).

When are these effects small? One expects the results of the previous sections to be weakly modified when $\omega L \gg [v_{Ti}, v]$. The main effect of the drift velocity is then to introduce a small modulation of the noise as a function of the angle θ between $\mathbf{v}$ and $\mathbf{Oz}$. From section 2.1, we expect the signal to be maximum when $\theta = 0$ for a small wire dipole satisfying $kL \ll 1$ or for a sphere dipole of any length; but for a wire dipole satisfying $kL \gg 1$, we expect it to be maximum at $\theta = \pi/2$. This is in agreement with a more formal derivation [*Meyer-Vernet et al.*, 1986a].

An important practical consequence is that a long ($L \gg L_D$) wire dipole should generally detect a noise maximum at $\theta = \pi/2$ for f of the order of magnitude of f_p; this behaviour, which is contrary to results [*Kellogg*, 1981] based on a "hand- waving" argument, has indeed been observed below f_p [*Meyer- Vernet et al.*, 1986a]. Note, however, that our argument is only qualitative: an explicit calculation must be done in order to get a firm answer. Then, the observed noise polarization can be used for deducing the direction of the velocity $\mathbf{v}$.

6.2.3 Magnetic field. When can we neglect the ambient static magnetic field $\mathbf{B}$?

Let $\Omega = eB/m$ and $\sigma = L_D\omega_p/\Omega$ be the electron gyrofrequency and gyroradius, respectively. Since we are only considering frequencies ω of the order of magnitude of ω_p, neglecting $\mathbf{B}$ requires $L_D \ll \sigma$, or $\Omega \ll \omega_p$.

How is the noise modified if this does not hold?

The problem is not simple, even in a thermal plasma, and in general the calculations only take into account the contribution of particular modes or directions of $\mathbf{k}$ [see *Sentman*, 1982] and skip the antenna geometry. Even so, they remain very complicated.

To illustrate the problem, consider first a thermal plasma, with $\Omega < \omega_p$ and $L_D < \sigma \ll L$.

Then, approximating the field as deriving from a scalar potential ($\omega \ll kc$), with $k\sigma \ll 1$, $\omega \gg kv_T$, and $\omega \neq n\Omega$ ("cold plasma"), one gets

$$k^2\epsilon_L \approx k_z^2\epsilon_1 + k_r^2\epsilon_2 + io \quad (35)$$

where $\epsilon_1 = 1 - \omega_p^2/\omega^2$, $\epsilon_2 = 1 - \omega_p^2/\left(\omega^2 - \Omega^2\right)$, and we have set $\mathbf{B} = \mathbf{e_z}B$ and $k^2 = k_z^2 + k_r^2$. As is well known, if $\Omega < \omega_p$, (35) has a zero only in the upper hybrid band:

$$\omega_p < \omega < \omega_{UH} = \left(\Omega^2 + \omega_p^2\right)^{1/2}$$

Inserting (35) in (11) and (12) gives for a dipole parallel to $\mathbf{B}$

$$V^2 = \frac{-4KT}{(2\pi)^3\epsilon_0\omega}\mathrm{Im}\int \mathbf{dk}\frac{k_z^2|J(\mathbf{k})|^2}{k_z^2\epsilon_1 + k_r^2\epsilon_2 + io} \quad (36)$$

Performing the k_z integration by residues, one obtains

$$V^2 = \frac{KT\beta}{\pi\epsilon_0\omega\epsilon_1}\int_0^\infty dk_r k_r^2 |J(k_r, \beta k_r)|^2 \quad (37)$$

where $\beta = (-\epsilon_2/\epsilon_1)^{1/2}$ and $J(\mathbf{k}) = J(k_r, k_z)$. Inserting (2) and (3), we get, if $a \ll \beta L$ and $\omega_p < \omega < \omega_{UH}$,

Wire dipole $\parallel \mathbf{B}$

$$V^2 = \frac{mv_T^2}{\epsilon_0\omega L|\epsilon_2|} \quad (38)$$

Sphere dipole

$$V^2 = \frac{mv_T^2}{2\epsilon_0\omega a[\epsilon_2(\epsilon_2 - \epsilon_1)]^{1/2}} \quad (39)$$

Because of the cold plasma approximation, this assumes $\omega \neq n\Omega$ and respectively $[a, \sigma] \ll [L, \beta L]$ for (38), or $[\sigma, \beta\sigma] \ll a\left(1 + \beta^2\right)^{1/2} \ll \beta L$ for (39). Thus, while (38) applies to long thin wire dipoles, (39) is less useful since it requires large sphere radii.

Thus, for long thin wire dipoles, we get a noise peak just below ω_{UH}, i.e.

$$V^2 \approx 1{\cdot}6V_0^2\omega_p^2/\left(\omega_{UH}^2 - \omega^2\right)$$

for $\left(\omega_{UH}^2 - \omega^2\right) \gg \left(\omega_p^2/\omega_{UH}\right)^2 (L_D/L)^2$ (where V_0^2 is defined in Table 1), which behaves much like the peak above ω_p in an isotropic plasma. For $\omega \approx \omega_p$, (38) yields $V^2 \approx V_0^2\left[(\omega_p/\Omega)^2 - 1\right]$.

Taking into account more correctly the plasma finite temperature does not change very much those results in the frequency band $\Omega < \omega_p < \omega < \omega_{UH}$, for long ($L \gg \sigma$) wire dipoles [*Meyer and Vernet*, 1974; *Nakatani and Kuehl*, 1976]. Outside this band, V^2 decreases smoothly above ω_{UH} if $\omega \neq n\Omega$, and for $\omega \gg \omega_p$, it joins the results in an isotropic plasma (Table 1).

Now, let us take as in section 5 a plasma with both a cold (C) and a hot (H) Maxwellian population. Assuming $\omega L/v_{TH} \gg 1$, $\omega \neq n\Omega$, one develops $\epsilon_L(k, \omega)$ and $E_{zz}(k, \omega)$ [*Sitenko*, 1967] for $k\sigma_P \ll 1$ and $(\omega - n\Omega)/|k_z|v_{TP} \gg 1$ with $P = C, H$, to obtain, instead of (35) and (36),

$$k^2\epsilon_L = k_z^2\epsilon_1 + k_r^2\epsilon_2 + i\pi^{1/2}\sum_P z_P e^{-z_P^2}/L_{DP}^2 \quad (40)$$

$$V^2 = \frac{K}{2\pi^{5/2}\epsilon_0\omega}\int \mathbf{dk}\frac{k_z^2|J(\mathbf{k})|^2}{|k^2\epsilon_L|^2} \times \sum_P T_P z_P e^{-z_P^2}/L_{DP}^2 \quad (41)$$

where $\epsilon_1 = 1 - \omega_{pT}^2/\omega^2$, $\epsilon_2 = 1 - \omega_{pT}^2/\left(\omega^2 - \Omega^2\right)$, $z_P = \omega/|k_z v_{TP}|$, and $\beta = (-\epsilon_2/\epsilon_1)^{1/2}$.

In the upper hybrid band defined by

$$\omega_{pT} < \omega < \left(\omega_{pT}^2 + \Omega^2\right)^{1/2}$$

the (dominant) contribution of the pole is

$$V^2 = \frac{\beta KT_C}{\pi\epsilon_0\omega\epsilon_1}\int_0^\infty dk_r k_r^2 |J(k_r, \beta k_r)|^2 \times \frac{1 + C\alpha t^{-1/2}}{1 + C\alpha t^{-3/2}} \quad (42)$$

with $C = \exp\left[\omega^2(1 - 1/t)/(\beta k_r v_{TC})^2\right]$ (compare with (29)). The main contribution to the integral stems from $\beta k_r > 1/L$; thus $C \gg 1$ (since $\omega L/v_{TC} \gg 1$). Hence, (42) reduces to (38) (wires) and/or (39) (spheres) multiplied by the factor t.

Now, let us take an antenna making an angle $\theta \neq 0$

with **B**. In general, this does not change the results for the long double sphere antenna. For the long wire, equations (36) and (41) can easily be generalized by replacing the components k_z and k_τ in the factor $\left[k_z^2 |J(\mathbf{k})|^2\right]$ by the components of **k** parallel and perpendicular, respectively, to the antenna. Using (36) and integrating as previously in cylindrical coordinates, we obtain an angular integration of the form $\int d\phi / Den(\phi)$ in the domain $Den(\phi) = |\cos\theta + \sin\theta \cos\phi/\beta| > a\left(1+\beta^{-2}\right)/L$. Besides, if the plasma contains two electron populations, then the integrand is multiplied by t when $Den(\phi) > v_{TC}/\omega L$. We get finally the approximate result

if $M > 0$

$$V^2 = \frac{m v_{TC}^2 t}{\epsilon_0 \omega L |\epsilon_2| |M|^{1/2}} \tag{43}$$

if $M < 0$

$$V^2 = \frac{m v_{TC}^2 t}{\epsilon_0 \omega L |\epsilon_2| |M|^{1/2}} \times (2/\pi) \ln\left[\frac{-2\beta M \omega L}{v_{TC} \sin\theta}\right] \tag{44}$$

where $M = \cos^2\theta - \sin^2\theta/\beta^2 \neq 0$, $\beta \neq 0$. If the plasma is Maxwellian ($t = 1$), then v_{TC}/ω is to be replaced by $a\left(1+\beta^{-2}\right)^{1/2}$ in the logarithmic term and (43) and (44) reduce to a classic impedance result [*Balmain*, 1964].

In short, if the antenna makes an angle $\theta \neq 0$ with the magnetic field, the noise peak on a long ($L > \sigma$) wire dipole at $\omega \approx \omega_{UH}$ is smaller than for $\theta = 0$; there is an additional peak at the frequency ω_R satisfying $\beta = \tan\theta$, and the noise is larger between ω_R and ω_{UH} than in the remaining part of the upper hybrid band. It is important to remember that, as we noted for $\theta = 0$, V^2 is much smaller but not necessarily negligible outside the upper hybrid band, as shown by taking more correctly the plasma temperature into account (see also *Meyer-Vernet* [1978]). We emphasise that the above results hold only for a long antenna: otherwise the contribution of the Bernstein modes becomes important [see *Sentman*, 1982].

7 CONCLUSIONS

For electron diagnosis by (quasi) thermal noise spectroscopy around the plasma frequency, the best antenna is a long ($L \gg L_D$ or at least $L >$ a few L_D) thin wire dipole. The low-frequency level gives the cold temperature, the high-frequency level gives the total electron pressure, the cutoff frequency gives the total density, and the shape of the peak gives the other parameters (see sections 4.3 or 5.3). A gap and/or an angle between the antenna arms does not change the diagnosis of those first three parameters provided that $L \gg L_D$; we emphasise that this is not true for intermediate lengths and that the diagnosis of the other parameters is then modified for any length.

If $L \gg L_D$, a small ($v \ll \omega L$) drift velocity produces a small noise variation (if the ion thermal velocity is smaller than ωL) with the angle between **v** and the wires, which can be used for deducing the direction of **v**. Remember that the polarization (on a long wire dipole) differs by $\pi/2$ from that on a small dipole.

If $L \gg L_D$, a magnetic field does not change those results if $\Omega \ll \omega_p$. For larger magnetic fields, but $\Omega < \omega_p$ and $L \gg \sigma$, the peak near the upper hybrid frequency behaves nearly like that for $\mathbf{B} = 0$ if the wires are parallel to **B**.

This toolkit can be used in particular in the following media.

1. The solar wind. The magnetic field is negligible; the drift velocity **v** causes a very small noise variation, except at distances larger than about 10 AU, where the inequality $\omega_p L/v \gg 1$ no longer holds for a typical antenna because of the small density: in the latter case, the antenna resistance may be negative if $v > v_T$, possibly causing an antenna instability and noise amplification. Note in passing that one can ask whether the emission detected in the distant solar wind [*Kurth et al.*, 1984] and attributed to a radiation coming from the outer boundary of the heliosphere is due instead to a negative antenna resistance when the phase in the solar cycle and/or the distance to the Sun ensure both $v > v_T$ and $\omega_p L/v_T \leq 1$.

2. Cometary plasmas. Both the magnetic field and the drift velocity are negligible; furthermore, in the comet coma and tail the high density and/or low temperature yield a small Debye length, so that it is not very difficult to get a "long" antenna.

3. Planetary ionospheres and inner magnetospheres, and the Io torus. The drift velocity is negligible, but in general the magnetic field is not. Fortunately, the Debye length is generally small, so that one easily gets a "long antenna"; then, section 6.2.3 gives a rough approximation.

We have skipped the following important problems:

1. It is well known that suprathermal electrons can seldom be represented by a Maxwellian component; how does this change the above results? In other words, what are the model-independent quasi-thermal noise features? Do they exist at all? This question is presently under study. A related point is the behaviour when the distribution function is marginally stable.

2. What happens when the antenna dc potential is large compared with the electron thermal energy, as should occur for the proposed "Tether" experiment [*Dobrowolny*, 1987] or the space station projects? Then, the disturbed plasma sheath surrounding the antenna changes significantly the impedance (see, for instance, *Calder and Laframboise*, [1985]). For large positive antenna potential, the consequently large electron transit time in the sheath can even produce a negative resistance and noise amplification, as recently shown in the laboratory [*Stenzel*, 1987].

We hope that this toolkit will help geophysicists to first consider the (simple?) plasma quasi-thermal noise or an intrinsic antenna instability before "discovering" a new noise or plasma instability.

Acknowledgments. The numerical results of this paper are based on a computer program written by P. Couturier. We thank our colleagues at Meudon Observatory for a critical reading, and especially Ludwik Celnikier for his help in improving this paper and for sharing his skills in taming the menagerie of TEX's procedures without getting eaten.

The editor thanks A. C. Calder and D. D. Sentman for their assistance in evaluating this paper.

REFERENCES

Andronov, A. A., Antenna impedance and noise in a space plasma (in Russian), *Kosm. Issled.*, *4*, 558, 1966.

Balmain, K. G., The impedance of a short dipole antenna in a magnetoplasma, *IEEE Trans. Antennas Propag.*, *AP-12*, 605, 1964.

Balmain, K. G., Impedance of a short dipole in a compressible plasma, *J. Res. Nat. Bur. Stand., Sect. D*, *69*, 559, 1965.

Birmingham, T. J., J. K. Alexander, M. D. Desch, R. F. Hubbard, and B. M. Pedersen, Observations of electron gyroharmonic waves and the structure of Io torus, *J. Geophys. Res., 86*, 8497, 1981.

Brown, L. W., The galactic radio spectrum between 130 and 2600 kHz, *Astrophys. J., 180*, 359, 1973.

Calder, A. C., and J. G. Laframboise, Terminal properties of a spherical RF electrode in an isotropic Vlasov plasma: Results of a computer simulation, *Radio Sci., 20*, 989, 1985.

Couturier, P., S. Hoang, N. Meyer-Vernet, and J. L. Steinberg, Quasi-thermal noise in a stable plasma at rest, *J. Geophys. Res., 86*, 11,127, 1981.

De Pazzis, O., Shot noise in antennas, *Radio Sci., 4*, 91, 1969.

Dobrowolny, M., The TSS project: Electrodynamics of long metallic tethers in the ionosphere, *Riv. Nuovo Cimento, 10*, 1, 1987.

Fejer, J. A., and J. R. Kan, Noise spectrum received by an antenna in a plasma, *Radio Sci., 4*, 721, 1969.

Fiala, V., Resistance of a plane grid condenser moving through a plasma, *IEEE Trans. Antennas Propag., AP-18*, 834, 1970.

Ginzburg, V. L., *Theoretical Physics and Astrophysics*, Pergamon, New York, 1979.

Harvey, C. C., J. Etcheto, and A. Mangeney, Early results from the ISEE Electron Density Experiment, *Space Sci. Rev., 23*, 39, 1979.

Hoang, S., J. L. Steinberg, G. Epstein, P. Tilloles, J. Fainberg, and R. G. Stone, The low-frequency continuum as observed in the solar wind from ISEE 3: Thermal electrostatic noise, *J. Geophys. Res., 85*, 3419, 1980.

Kellogg, P. J., Calculation and observation of thermal electrostatic noise in solar wind plasma, *Plasma Phys., 23*, 735, 1981.

Kuehl, H. H., Resistance of a short antenna in a warm plasma, *Radio Sci., 1*, 971, 1966.

Kuehl, H. H., Computations of the resistance of a short antenna in a warm plasma, *Radio Sci., 2*, 73, 1967.

Kurth, W. S., D. A. Gurnett, F. L. Scarf, and R. L. Poynter, Detection of a radio emission at 3 kHz in the outer heliosphere, *Nature, 312*, 27, 1984.

Laframboise, J. G., and L. W. Parker, Probe design for orbit-limited current collection, *Phys. Fluids, 16*, 629, 1973.

Meyer, P., and N. Vernet, Impedance of a short antenna in a warm magnetoplasma, *Radio Sci., 9*, 409, 1974.

Meyer-Vernet, N., Impedance of a short antenna in a warm magnetoplasma: Experiment and comparison with theory, *Radio Sci., 13*, 1059, 1978.

Meyer-Vernet, N., On natural noises detected by antennas in plasmas, *J. Geophys. Res., 84*, 5373, 1979.

Meyer-Vernet, N., Quasi-thermal noise corrections due to particle impacts or emission, *J. Geophys. Res., 88*, 8081, 1983*a*.

Meyer-Vernet, N., Grain spin-up by inverse Cerenkov effect, *Astron. Astrophys., 119*, 117, 1983*b*.

Meyer-Vernet, N., P. Couturier, S. Hoang, and J. L. Steinberg, Ion thermal noise in the solar wind: Interpretation of the "excess" electric noise on ISEE 3, *J. Geophys. Res., 91*, 3294, 1986*a*.

Meyer-Vernet, N., P. Couturier, S. Hoang, C. Perche, J. L. Steinberg, J. Fainberg, and C. Meetre, Plasma diagnosis from thermal noise and limits on dust flux or mass in comet Giacobini-Zinner, *Science, 232*, 370, 1986*b*.

Meyer-Vernet, N., P. Couturier, S. Hoang, C. Perche, and J. L. Steinberg, Physical parameters for hot and cold electron populations in comet Giacobini-Zinner with the ICE radio experiment, *Geophys. Res. Lett., 13*, 279, 1986*c*.

Nakatani, D. T., and H. H. Kuehl, Input impedance of a short dipole antenna in a warm anisotropic plasma, 1, Kinetic theory, *Radio Sci., 11*, 433, 1976.

Schiff, M. L., Impedance of a short dipole antenna in a warm isotropic plasma, *Radio Sci., 5*, 1489, 1970.

Schiff, M. L., and J. A. Fejer, Impedance of antennas in a warm isotropic plasma: A comparison of different models, *Radio Sci., 5*, 811, 1970.

Sentman, D. D., Thermal fluctuations and the diffuse electrostatic emissions, *J. Geophys. Res., 87*, 1455, 1982.

Shaw, R. R., and D. A. Gurnett, Electrostatic noise bands associated with the gyrofrequency and plasma frequency in the outer magnetosphere, *J. Geophys. Res., 80*, 4259, 1975.

Sitenko, A. G., *Electromagnetic Fluctuations in Plasma*, Academic, San Diego, Calif., 1967.

Steinberg, J. L., and S. Hoang, Electric noise observations with the ISEE-3 radio receiver: Thermal noise and the $2f_p$ line from the Lagrange point to $14R_E$ from the earth, *Ann. Geophys., Ser. A, 4*, 429, 1986.

Stenzel, R. L., Instability of the sheath-plasma resonance, *Phys. Rev. Lett., 60*, 704, 1987.

N. Meyer-Vernet and C. Perche, CNRS URA 667, Observatoire de Meudon, 92195 Meudon Principal Cedex, France.

(Received April 11, 1988;
revised June 28, 1988;
accepted June 28, 1988)